

Mechanistic Information from Low-Temperature Rapid-Scan and NMR Measurements on the Protonation and Subsequent Reductive Elimination Reaction of a (Diimine)platinum(II) Dimethyl Complex

Bror J. Wik,[†] Ivana Ivanovic-Burmazovic,[‡] Mats Tilset,^{*,†} and Rudi van Eldik^{*,‡}

Department of Chemistry, University of Oslo, P.O. Box 1033, Blindern, N-0315 Oslo, Norway, and Institute for Inorganic Chemistry, University of Erlangen-Nürnberg, Egerlandstrasse 1, 91058 Erlangen, Germany

Received November 11, 2005

A detailed kinetic study of the protonation and subsequent reductive elimination reaction of a (diimine)platinum(II) dimethyl complex was undertaken in dichloromethane over the temperature range of -90 to $+10$ °C by stopped-flow techniques. Time-resolved UV–vis monitoring of the reaction allowed the assessment of the effects of acid concentration, coordinating solvent (MeCN) concentration, temperature, and pressure. The second-order rate constant for the protonation step was determined to be $15200 \pm 400 \text{ M}^{-1} \text{ s}^{-1}$ at -78 °C, and the corresponding activation parameters are $\Delta H^\ddagger = 15.2 \pm 0.6 \text{ kJ mol}^{-1}$ and $\Delta S^\ddagger = -85 \pm 3 \text{ J mol}^{-1} \text{ K}^{-1}$, which are in agreement with the addition of a proton that results in the formation of the platinum(IV) hydrido complex. The kinetics of the second, methane-releasing reaction step do not show an acid dependence, and the MeCN concentration also does not significantly affect the reaction rate. The activation parameters for the second reaction step were found to be $\Delta H^\ddagger = 75 \pm 1 \text{ kJ mol}^{-1}$, $\Delta S^\ddagger = +38 \pm 5 \text{ J mol}^{-1} \text{ K}^{-1}$, and $\Delta V^\ddagger = +18 \pm 1 \text{ cm}^3 \text{ mol}^{-1}$, strongly suggesting a dissociative character of the rate-determining step for the reductive elimination reaction. The spectroscopic and kinetic observations were correlated with NMR data and assisted the elucidation of the underlying reaction mechanism.

Introduction

The development of direct, selective methods for catalytic conversion of hydrocarbons to value-added products remains a significant challenge.^{1–4} Early work by Garnett and Shilov established that aqueous Pt^{II} salts are capable of activating C–H bonds of arenes and alkanes.^{5–7} Mechanistic studies on the aqueous K₂PtCl₄ system and on model systems have

provided significant mechanistic insight, and the activation and functionalization of hydrocarbons in the “Shilov system” are considered to take place by the general mechanism depicted in Scheme 1.^{8–10}

We and others^{11–24} have recently carried out a series of mechanistic studies pertaining to the C–H activation steps

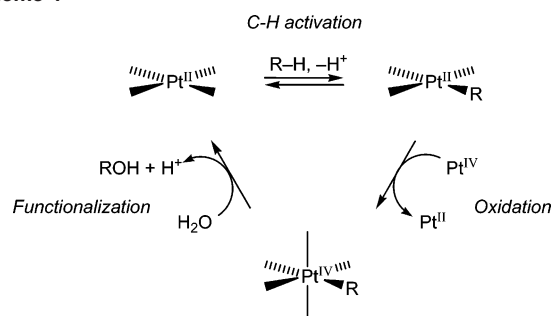
* To whom correspondence should be addressed. E-mail: mats.tilset@kjemi.uio.no (M.T.), vaneldik@chemie.uni-erlangen.de (R.v.E.).

[†] University of Oslo.

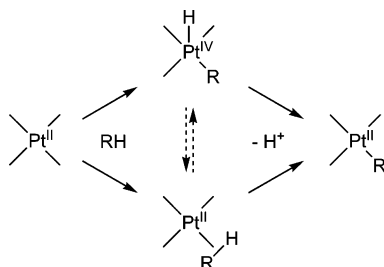
[‡] University of Erlangen-Nürnberg.

- Labinger, J. A.; Bercaw, J. E. *Nature* **2002**, *417*, 507–514.
- Shilov, A. E.; Shul'pin, G. B. *Activation and catalytic reactions of saturated hydrocarbons in the presence of metal complexes*; Kluwer Academic: Dordrecht, The Netherlands, 2000.
- Crabtree, R. H. *J. Chem. Soc., Dalton Trans.* **2001**, 2437–2450.
- Arndtsen, B. A.; Bergman, R. G.; Mobley, T. A.; Peterson, T. H. *Acc. Chem. Res.* **1995**, *28*, 154–162.
- Garnett, J. L.; Hodges, R. J. *J. Am. Chem. Soc.* **1967**, *89*, 4546–4547.
- Gol'dshleger, N. F.; Shteinman, A. A.; Shilov, A. E.; Eskova, V. V. *Zh. Fiz. Khim.* **1972**, *46*, 1353–1354.
- Gol'dshleger, N. F.; Tyabin, M. B.; Shilov, A. E.; Shteinman, A. A. *Zh. Fiz. Khim.* **1969**, *43*, 2174–2175.
- Lersch, M.; Tilset, M. *Chem. Rev.* **2005**, *105*, 2471–2526.
- Fekl, U.; Goldberg, K. I. *Adv. Inorg. Chem.* **2003**, *54*, 259–320.
- Stahl, S. S.; Labinger, J. A.; Bercaw, J. E. *J. Am. Chem. Soc.* **1996**, *118*, 5961–5976.
- Heiberg, H.; Johansson, L.; Gropen, O.; Ryan, O. B.; Swang, O.; Tilset, M. *J. Am. Chem. Soc.* **2000**, *122*, 10831–10845.
- Johansson, L.; Tilset, M.; Labinger, J. A.; Bercaw, J. E. *J. Am. Chem. Soc.* **2000**, *122*, 10846–10855.
- Johansson, L.; Tilset, M. *J. Am. Chem. Soc.* **2001**, *123*, 739–740.
- Johansson, L.; Ryan, O. B.; Rømming, C.; Tilset, M. *J. Am. Chem. Soc.* **2001**, *123*, 6579–6590.
- Wik, B. J.; Lersch, M.; Tilset, M. *J. Am. Chem. Soc.* **2002**, *124*, 12116–12117.
- Zhong, H. A.; Labinger, J. A.; Bercaw, J. E. *J. Am. Chem. Soc.* **2002**, *124*, 1378–1399.
- Procelewska, J.; Zahl, A.; van Eldik, R.; Zhong, H. A.; Labinger, J. A.; Bercaw, J. E. *Inorg. Chem.* **2002**, *41*, 2808–2810.
- Heyduk, A. F.; Labinger, J. A.; Bercaw, J. E. *J. Am. Chem. Soc.* **2003**, *125*, 6366–6367.

Scheme 1



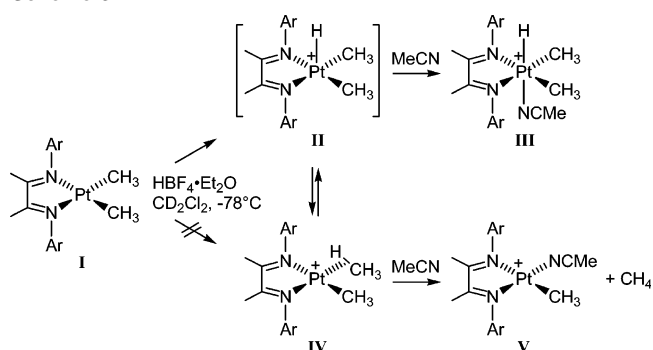
Scheme 2



using model complexes $(\text{N}-\text{N})\text{PtR}_2$, where $\text{N}-\text{N}$ is a diimine ligand. One question that has been addressed^{15,25} is whether the proton to be removed from the hydrocarbon dissociates directly from an activated metal–hydrocarbon complex (a so-called σ complex) or from a hydrido ligand that is formed via oxidative cleavage of the C–H bond of the σ -complex intermediate (Scheme 2). The fact that scrambling of isotope labels occurs^{11–13,16,25} between hydrido and alkyl sites demonstrates that these species interconvert in solution and complicates probing of the true, kinetically preferred site of deprotonation.

The question of the site of deprotonation was recently addressed by us by investigating the reverse reaction, i.e., protonation of $(\text{N}-\text{N})\text{PtMe}_2$ (**I**; Scheme 3).¹⁵ Protonation might occur either at a coordinated methyl ligand to produce the transient σ -methane complex (**IV**, bottom) or at the metal (top), resulting in a transient pentacoordinate platinum(IV) hydridodimethyl species (**II**). Either of these species is expected to be trapped by an added ligand, in this case acetonitrile, in an associative fashion^{12–14,17} to produce the platinum(II) solvento complex **V** or the hexacoordinate platinum(IV) solvento complex **III**, respectively. (The protonation and acetonitrile ligation at Pt may also occur in a concerted fashion, which will be equally consistent with our analysis.) Protonation of $(\text{N}-\text{N})\text{PtMe}_2$ in deuterated dichloromethane (CD_2Cl_2) at -78°C in the presence of MeCN led to mixtures of $(\text{N}-\text{N})\text{Pt}^{\text{II}}(\text{Me})(\text{NCMe})^+$ (plus methane)

Scheme 3



and $(\text{N}-\text{N})\text{Pt}^{\text{IV}}(\text{Me})_2(\text{H})(\text{NCMe})^+$. Increasing concentrations of MeCN led to reduced $\text{Pt}^{\text{II}}/\text{Pt}^{\text{IV}}$ product ratios. This is consistent with protonation occurring mostly, if not exclusively, at Pt rather than at a methyl group and also demonstrates that, under the reaction conditions, C–H reductive coupling and trapping by the added MeCN ligand occur at comparable rates.¹⁵

However, no quantitative data have been available on the kinetics of the protonation step and the accompanying MeCN trapping starting from $(\text{N}-\text{N})\text{PtMe}_2$. In this paper, we report the details of a kinetic study of these reactions. Concentration-, temperature-, and pressure-dependent kinetic measurements allow us to evaluate the kinetics of the protonation and trapping of MeCN at low temperatures and of MeCN dissociation and C–H reductive coupling at higher temperatures.

Experimental Section

General Considerations. Solvents for the kinetic measurements were used without further purification. P.a.-grade and ultradry acetonitrile and CH_2Cl_2 were supplied by Acros. The measurements in p.a. grade and ultradry solvents did not show any significant differences. The specific complex studied in this work, $(\text{N}'-\text{N}')\text{PtMe}_2$, where the diimine $\text{N}'-\text{N}'$ is $\text{ArN}=\text{C}(\text{Me})-\text{C}(\text{Me})=\text{NAr}$ with $\text{Ar} = 2,6\text{-Me}_2\text{C}_6\text{H}_3$, was synthesized according to reported methods¹² from $[\text{Me}_2\text{Pt}(\mu\text{-SMe}_2)]_2$ ²⁶ and the diimine.²⁷

Sample Preparation. In the kinetic studies, two different protocols were used for the preparation of the solutions of the Pt complex $(\text{N}'-\text{N}')\text{PtMe}_2$ and the acid $\text{HBF}_4\cdot\text{Et}_2\text{O}$. In one protocol, a solution of the Pt complex in neat CH_2Cl_2 was mixed with the acid solution, which was premade in $\text{MeCN}/\text{CH}_2\text{Cl}_2$ solvent mixtures to yield the desired concentrations of acid, MeCN, and $(\text{N}'-\text{N}')\text{PtMe}_2$ after mixing. Using this procedure, different experiments were conducted in which the acid concentration was varied at a constant concentration of MeCN or vice versa. In the other protocol, CH_2Cl_2 solutions of the Pt complex and of the acid were separately prepared with the appropriate concentration of MeCN being present in *both* solutions. Thus, in the study of the acetonitrile dependence of the kinetics, a new solution of the acid as well as the complex had to be prepared for each set of measurements. In the observation cell, the concentration of $(\text{N}'-\text{N}')\text{PtMe}_2$ was 0.125 mM, whereas the acid concentration was varied between 0.5 and 3 mM, and the concentration of acetonitrile was adjusted to be between 1 and 30 vol % after mixing. A series of experiments with

(19) Heyduk, A. F.; Driver, T. G.; Labinger, J. A.; Bercaw, J. E. *J. Am. Chem. Soc.* **2004**, *126*, 15034–15035.

(20) Driver, T. G.; Day, M. W.; Labinger, J. A.; Bercaw, J. E. *Organometallics* **2005**, *24*, 3644–3654.

(21) Gerdes, G.; Chen, P. *Organometallics* **2003**, *22*, 2217–2225.

(22) Labinger, J. A.; Bercaw, J. E.; Tilset, M. *Organometallics* **2006**, *25*, 805–808.

(23) Gerdes, G.; Chen, P. *Organometallics* **2006**, *25*, 809–811.

(24) Wik, B. J.; Lersch, M.; Krivokapic, A.; Tilset, M. *J. Am. Chem. Soc.* **2006**, *128*, 2682–2696.

(25) Tilset, M.; Johansson, L.; Lersch, M.; Wik, B. J. *ACS Symp. Ser.* **2004**, *885*, 264–282.

(26) Scott, J. D.; Puddephatt, R. J. *Organometallics* **1983**, *2*, 1643–1648.

(27) Tom Dieck, H.; Svoboda, M.; Greiser, T. *Z. Naturforsch. B* **1981**, *36B*, 823–832.

different concentrations of Bu₄NPF₆ were performed in order to check whether the ionic strength of the solution influences the protonation reaction. The ionic strength did not show any significant effects on the rate of the reaction up to 3 mM Bu₄NPF₆.

Measurements. UV-vis spectra were recorded on Shimadzu UV-2101 and Hewlett-Packard 8542A spectrophotometers. Low-temperature kinetic data were obtained by recording time-resolved UV-vis spectra using a modified Bio-Logic stopped-flow module μ SFM-20 combined with a cryo-stopped-flow accessory (Huber CC90 cryostat) and equipped with a J & M TIDAS high-speed diode array spectrometer with a combined deuterium and tungsten lamp (200–1015-nm bandwidth). Isolast O rings were used for all sealing purposes. Data were analyzed using the integrated Bio-Kine software, version 4.23, and the software package Specfit/32 global analysis program. Measurements under high pressure were carried out using a homemade high-pressure stopped-flow instrument,^{28,29} for which Isolast O rings were also used for all syringe seals.

At least 10 kinetic runs were recorded under all conditions, and the reported rate constants represent the mean values. The UV-vis spectrophotometers and stopped-flow instrument were thermostated to the desired temperature ± 0.1 °C. Values of ΔH^\ddagger and ΔS^\ddagger were calculated from the slopes and intercepts of plots of $\ln(k/T)$ versus $1/T$, respectively, and values of ΔV^\ddagger were calculated from the slope of plots of $\ln(k)$ versus pressure in the usual way.³⁰ The activation parameters and corresponding error limits were calculated from a weighted linear least-squares fit of the data, in which the experimental points were weighed according to the magnitude of the error (Origin version 7).

Check for H/D Scrambling in Unreacted Pt Methyl Groups by ¹H NMR. An NMR tube equipped with a Teflon needle valve was loaded with (N'-N')PtMe₂ (5 mg, 9.7×10^{-3} mmol), and CD₃-CN/CD₂Cl₂ (1:1, v/v; ca. 0.4 mL) was added by vacuum transfer. The tube was shaken to dissolve the content, and an ambient-temperature NMR spectrum (200 MHz) was recorded: δ 0.63 (s, ²J(¹⁹⁵Pt-H) = 86.7 Hz, 6 H, Pt-Me), 1.23 (s, 6 H, N=CMe), 2.11 (s, 12 H, aryl-Me), 6.98–7.21 (m, 6 H, aryl-H). The tube was immersed in a -45 °C cooling bath, and DOTf (9 μ L, ca. 10 equiv) was added against a flush of argon. The tube was quickly shaken to mix the reactants and held at the cooling bath temperature for 1.5 h. The ¹H NMR spectrum was then recorded at ambient temperature. The ¹H NMR spectrum (200 MHz) revealed the presence of CH₄ and CH₃D (ca. 1:1) as well as (N'-N')Pt(CH₃)-(NCCD₃)⁺: δ 0.14 (t, CH₃D), 0.15 (s, CH₄), 0.38 (s, ²J(¹⁹⁵Pt-H) = 75.2 Hz, 3 H, Pt-Me), 2.15 (s, 3 H, N=CMe), 2.25 (s, 3 H, N=CMe), 2.35 (s, 12 H, aryl-Me), 7.23–7.39 (m, 6 H, aryl-H). There was no detectable quantity of the isotopomer (N'-N')Pt-(CH₂D)(NCCD₃)⁺, which is readily¹³ discernible by ¹H NMR. There was also no evidence for D incorporation into the aryl-Me groups of the product or unreacted reactant. Protonation with HBF₄·Et₂O in the presence of small quantities of methanol-*d*₄ led to substantial amounts of CH₃D, demonstrating that isotopic "leakage" can occur with protic impurities.

Results and Discussion

The protonation of the platinum(II) dimethyl complex (N'-N')PtMe₂ with HBF₄·Et₂O in CD₂Cl₂ containing CD₃-

CN was previously studied by ¹H NMR spectroscopy.¹⁵ Protonation occurs at Pt with concomitant MeCN coordination to form the platinum(IV) hydrido complex (N'-N')Pt-(Me)₂(H)(NCMe)⁺, which is kinetically stabilized at low temperatures by the apically coordinated MeCN ligand.³¹ At temperatures of about -40 °C, a gradual release of methane and the formation of (N'-N')Pt(Me)(MeCN)⁺ were observed in a second reaction step. This reaction sequence has now been subjected to a systematic kinetic investigation in CH₂-Cl₂ containing variable amounts of MeCN over the temperature range of -90 to +10 °C by stopped-flow techniques with time-resolved UV-vis monitoring of the reaction. In general, the same two reaction steps are observed by UV-vis monitoring.

Protonation below -40 °C. The first reaction step was observed at -78 °C in MeCN/CH₂Cl₂ mixtures of different compositions (see the Experimental Section). The resulting time-resolved UV-vis spectra clearly indicate a one-step reaction as shown in Figure 1. The characteristic absorption bands of (N'-N')PtMe₂ at 540, 504, and 377 nm decay, while the absorbance at wavelengths below 320 nm increases, resulting in a clean isosbestic point at 320 nm. These spectral changes and the resulting pseudo-first-order kinetics do not depend on [MeCN] in the range of 5–30% (v/v). Lower acetonitrile concentrations could not be used for the kinetic measurements (but were utilized in the previous NMR study¹⁵) because of the decrease in solubility of HBF₄·Et₂O at low temperature.³² The presence of MeCN in the solution of (N'-N')PtMe₂ in CH₂Cl₂ prior to the addition of acid, or the addition of MeCN together with the acid, does not cause any differences in the spectra or the kinetics. To avoid potential complications arising from mixing of two different solvent compositions at low temperatures, it was preferable to have the same concentration of MeCN in both the solutions of the Pt complex and of the acid before mixing. The acid concentration dependence (0.5–3 mM acid) of the pseudo-first-order rate constants at -78 °C in the presence of 30% MeCN is shown in Figure 2. At the two lowest acid concentrations, the observed rate constants for protonation, $k_{\text{obs}}(\text{H}^+)$, were obtained from initial rate measurements because the kinetic traces exhibited a significant deviation from first-order behavior as a result of the absence of pseudo-first-order conditions. It appeared to us that the deviations may also be caused by incomplete acid or ion-pair dissociation to furnish the "free acid", whatever its exact identity might be,³³ under the low-temperature conditions. The initially rapid protonation caused by "free acid" would then be slowed at longer reaction times, either because further dissociation is needed to furnish the "free acid" or because protonation by "undissociated acid" does occur but at a considerably slower rate than that by "free acid". It is

(31) Puddephatt, R. J. *Coord. Chem. Rev.* **2001**, 219–221, 157–185.

(32) Triflic acid undergoes phase separation in CH₂Cl₂ at low temperatures: Bullock, R. M.; Song, J.-S.; Szalda, D. J. *Organometallics* **1996**, 15, 2504–2516.

(33) Protonated ether is the likely active proton donor because the approximate pK_a of protonated acetonitrile (ca. -12) is considerably lower than that of protonated ethers (-2 to -5): Lowry, T. H.; Richardson, K. S. *Mechanism and Theory in Organic Chemistry*; Harper & Row: New York, 1987; p 297.

(28) van Eldik, R.; Palmer, D. A.; Schmidt, R.; Kelm, H. *Inorg. Chim. Acta* **1981**, 50, 131–135.
(29) van Eldik, R.; Gaede, W.; Wieland, S.; Kraft, J.; Spitzer, M.; Palmer, D. A. *Rev. Sci. Instrum.* **1993**, 64, 1355–1357.
(30) van Eldik, R.; Hubbard, C. D. In *Chemistry at Extreme Conditions*; Riad Manaa, M., Ed.; Elsevier: Amsterdam, The Netherlands, 2005; Chapter 4, pp 109–164.

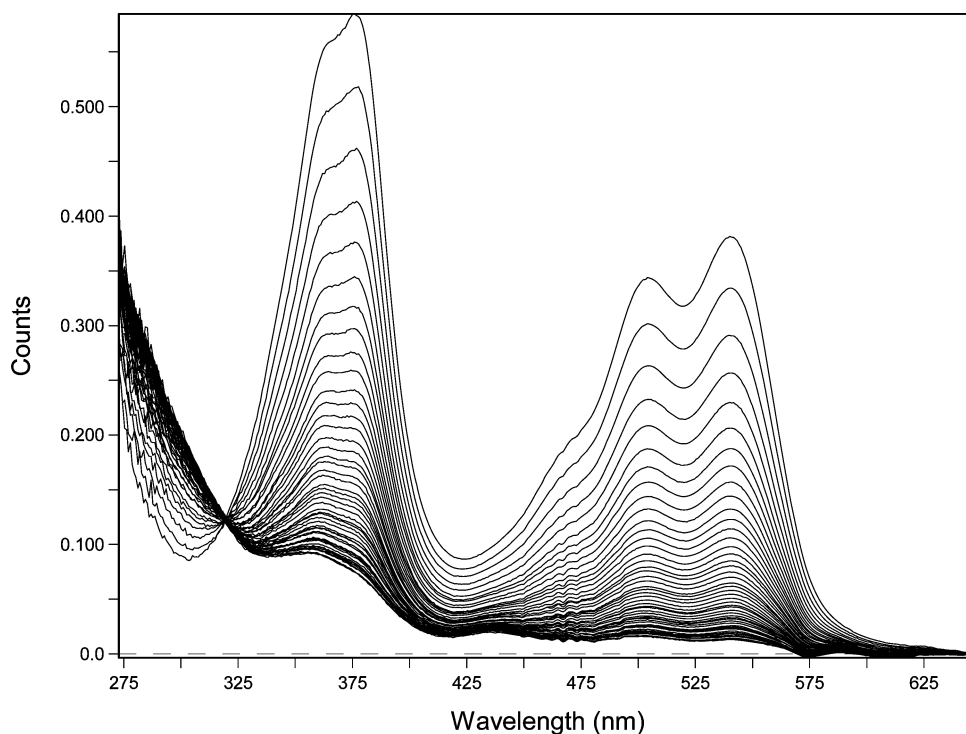


Figure 1. Time-resolved spectra for the protonation reaction of (N'-N')PtMe₂ in CH₂Cl₂ at -78 °C. Experimental conditions: [Pt^{II}] = 0.125 mM, [MeCN] = 5.74 M (30%), [HBF₄·Et₂O] = 1 mM, and reaction time = 0.6 s.

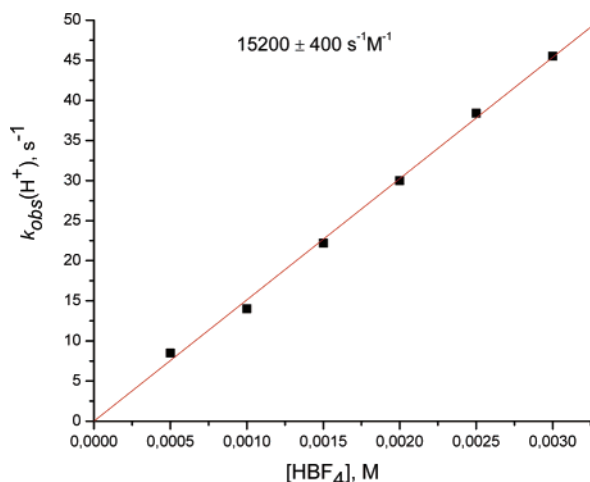


Figure 2. $k_{\text{obs}}(\text{H}^+)$ vs [HBF₄·Et₂O] for the protonation reaction in CH₂-Cl₂. Experimental conditions: [Pt^{II}] = 0.125 mM, [MeCN] = 5.74 M (30%), and $T = -78$ °C.

therefore important to have a substantially greater than 10-fold excess of acid compared to the (N'-N')PtMe₂ concentration in order to ensure a good first-order behavior. Because of the significant change in absorbance in the monitored UV-vis range caused by protonation of (N'-N')PtMe₂, the experiments could be performed with a lower concentration (0.03 mM) of the Pt complex at the lowest HBF₄·Et₂O concentrations (but unchanged MeCN concentrations), and indeed a clean first-order kinetic behavior resulted. To our gratification, under these conditions the $k_{\text{obs}}(\text{H}^+)$ value is in good agreement with the value obtained from the initial rates when operating at the higher Pt complex concentration. From the slope of the resulting good linear plot of $k_{\text{obs}}(\text{H}^+)$ versus [HBF₄·Et₂O] (Figure 2), the second-order rate constant for

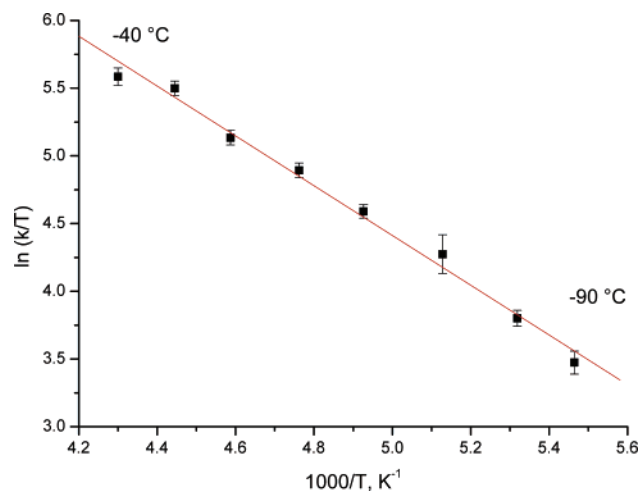


Figure 3. Eyring plot for the protonation of (N'-N')PtMe₂ with HBF₄·Et₂O in CH₂Cl₂. Experimental conditions: [Pt^{II}] = 0.125 mM, [MeCN] = 5.74 M (30%), and [HBF₄·Et₂O] = 1 mM.

the protonation step was found to be $15\,200 \pm 400 \text{ s}^{-1} \text{ M}^{-1}$ at -78 °C. The absence of a significant nonzero intercept suggests that there is no back or parallel reaction that is not first-order in [H⁺].

Temperature-dependent kinetic measurements (Table S1 in the Supporting Information) were done by recording the time-dependent spectra of the protonation of (N'-N')PtMe₂ with a 1 mM acid solution with 30% MeCN present in the temperature range of -90 to -40 °C. The rate constant $k_{\text{obs}}(\text{H}^+)$ could not be accurately obtained at higher temperatures because of the intervention of the subsequent reaction step (vide infra). The Eyring plot in Figure 3 shows an excellent linear fit, and the resulting activation parameters are $\Delta H^\ddagger = 15.2 \pm 0.6 \text{ kJ mol}^{-1}$ and $\Delta S^\ddagger = -85 \pm 3 \text{ J mol}^{-1} \text{ K}^{-1}$.

These appear to be rather unique data for the kinetic and activation parameters of protonation reactions at metal centers. Previous studies have revealed that protonation reactions of organotransition-metal complexes can be mechanistically complex. Protonation can occur at multiple sites in such complexes, either at the metal or at a ligand. There is a definite possibility that rapid proton transfer may occur, inter- or intramolecularly, between these sites, and this makes it far from trivial to assess which is the kinetically preferred site of protonation.^{34–38} It is commonly considered that proton transfers at carbon sites or at metal centers are intrinsically slow because of the considerable geometric and electronic rearrangements that arise as a consequence of the protonation event and that protonation of a hydrido ligand may be kinetically preferred because the accompanying structural/electronic changes are less significant.^{39–41} The protonation process described herein appears to be rather fast for a well-documented¹⁵ metal-centered process and is characterized by a low activation enthalpy. The large negative value for the activation entropy and the low activation enthalpy strongly suggest that the observed process has an associative character and is in agreement with the addition of a proton and MeCN, formally an oxidative addition process. This results in the formation of the platinum(IV) hydrido complex (N'–N')Pt(Me)₂(H)(NCMe)⁺, which, as already mentioned, was spectroscopically identified by ¹H NMR in the same temperature range and concluded to be the kinetically preferred protonation product.¹⁵ We infer that the product of our first reaction step has to be the hexacoordinate platinum(IV) hydrido complex, which is stabilized³¹ by the axial MeCN ligand.

The low-temperature protonation that was investigated by NMR¹⁵ was conducted at varying MeCN concentrations (see the Introduction). At low [MeCN], intramolecular reductive H–CH₃ coupling with subsequent associative methane displacement competed with MeCN trapping, concerted or stepwise, of the putative pentacoordinate intermediate (N'–N')Pt(Me)₂(H)⁺ to give a mixture of the Pt^{II} and Pt^{IV} complexes (N'–N')Pt(Me)(NCMe)⁺ and (N'–N')Pt(Me)₂(H)(NCMe)⁺, respectively, as products (Scheme 3). However, at higher [MeCN], trapping of the pentacoordinate species by MeCN was the predominant reaction pathway, and a rather clean formation of (N'–N')Pt(Me)₂(H)(NCMe)⁺ was observed. The stopped-flow kinetic experiments described herein were conducted at similarly high MeCN concentrations and, consequently, the Pt^{IV} product is the only observable product of the protonation step at –78 °C.

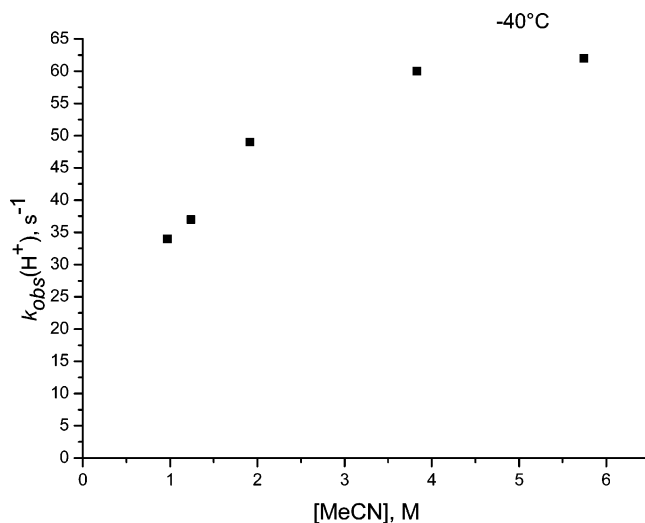


Figure 4. $k_{\text{obs}}(\text{H}^+)$ for the protonation reaction vs [MeCN] in CH₂Cl₂. Experimental conditions: [Pt^{II}] = 0.125 mM, [HBF₄·Et₂O] = 1 mM, and T = –40 °C.

Protonation above –40 °C. At –40 °C, a modest influence (less than a factor of 2) of [MeCN] on the observed rate constant for the protonation step, $k_{\text{obs}}(\text{H}^+)$, is observed when [MeCN] is varied from 0.95 to 5.9 M (Figure 4). Our interpretation of this, already discussed above in the context of low-temperature protonations at –78 °C, is that the increased solvent polarity will enhance acid or ion-pair dissociation to furnish the “free acid”. Hence, the effective “free acid” concentration will increase with increasing [MeCN] at constant [HBF₄·Et₂O] but only until complete dissociation is achieved. Only at –40 °C, when the protonation has become considerably faster than that at –78 °C, does the extent of dissociation start to affect the proton-transfer kinetics. Alternatively, the concentration dependence in Figure 4 might represent a “saturation effect” that is typical of saturation kinetics. Such behavior might result for a two-step protonation reaction in which MeCN is involved in the second step; i.e., capture of the pentacoordinate intermediate would be rate-limiting at low [MeCN]. Such behavior was, however, not seen at –78 °C, and it appears that the simplest unifying explanation for the [MeCN] dependence at all temperatures would be the acid/ion-pair dissociation model.

At –40 °C, the hexacoordinate platinum(IV) hydrido (N'–N')Pt(Me)₂(H)(NCMe)⁺ (based on the previous NMR studies¹⁵) undergoes a gradual methane release to furnish (N'–N')Pt(Me)(NCMe)⁺ sufficiently fast to be monitored together with the protonation step on the same time scale. In Figure 5a, a rapid decay of the absorbances at 544, 509, and 369 nm, which is characteristic for the conversion of the starting platinum(II) complex to the hexacoordinate platinum(IV) hydrido complex, is followed by a slow increase in absorbance at 397 and 306 nm related to the formation of the Pt^{II} product (N'–N')Pt(Me)(NCMe)⁺. The calculated spectra of the three Pt species involved in the two-step reaction mechanism are presented in Figure 5b, clearly depicting the individual spectra of starting, intermediate, and product complexes. On an even longer time scale, the second reaction step goes to completion (Figure 5c).

(34) Autissier, V.; Brockman, E.; Clegg, W.; Harrington, R. W.; Henderson, R. A. *J. Organomet. Chem.* **2005**, *690*, 1763–1771.

(35) Autissier, V.; Clegg, W.; Harrington, R. W.; Henderson, R. A. *Inorg. Chem.* **2004**, *43*, 3098–3105.

(36) Henderson, R. A.; Oglieve, K. E. *Chem. Commun.* **1999**, 2271–2272.

(37) Henderson, R. A. *Angew. Chem., Int. Ed. Engl.* **1996**, *35*, 946–967.

(38) Papish, E. T.; Rix, F. C.; Spetseris, N.; Norton, J. R.; Williams, R. D. *J. Am. Chem. Soc.* **2000**, *122*, 12235–12242.

(39) Kristjansdottir, S. S.; Norton, J. R. In *Transition Metal Hydrides*; Dedieu, A., Ed.; VCH: Weinheim, Germany, 1992; pp 309–359.

(40) Jessop, P. G.; Morris, R. H. *Coord. Chem. Rev.* **1992**, *121*, 155–284.

(41) Heinekey, D. M.; Oldham, W. J., Jr. *Chem. Rev.* **1993**, *93*, 913–926.

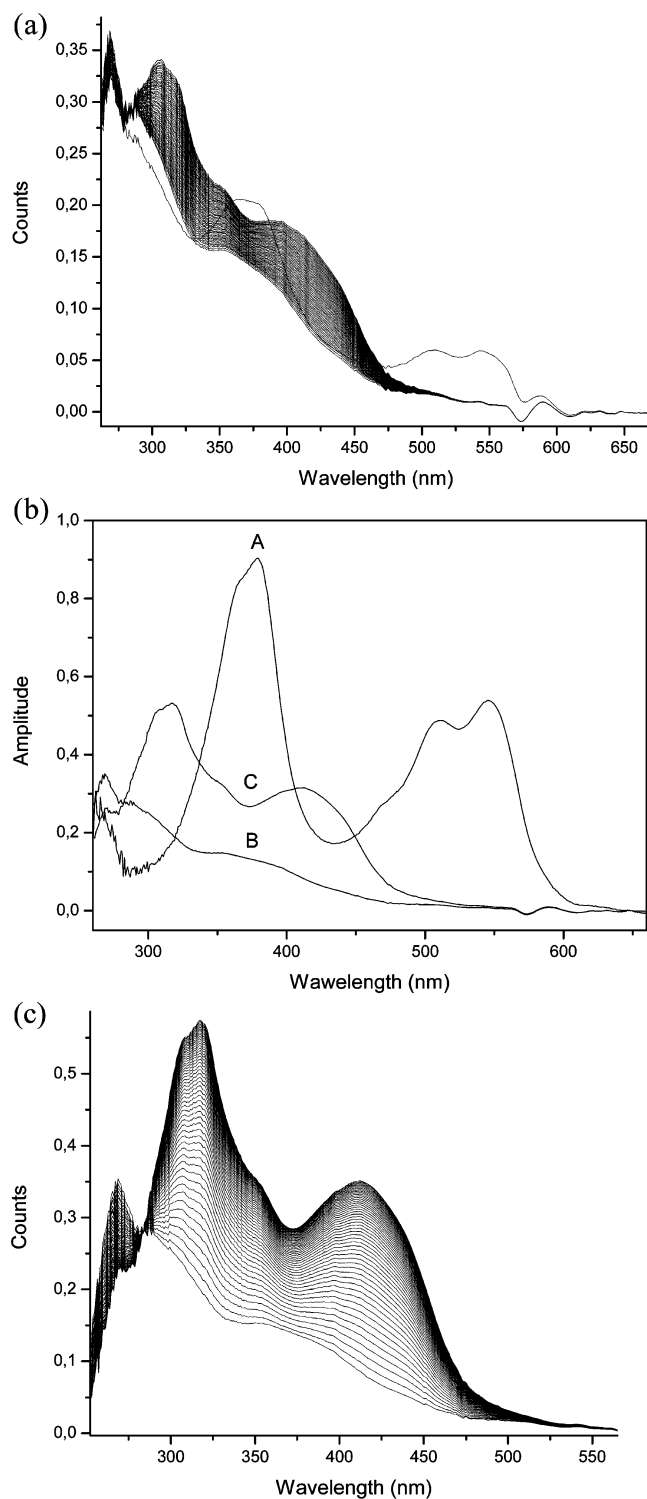


Figure 5. Time-resolved spectra for the reaction of (N'-N')PtMe₂ with HBF₄·Et₂O in CH₂Cl₂ at -40 °C. (a) Time scale: 1 min. (b) UV-vis spectra of (N'-N')PtMe₂ (A), intermediate (B), and (N'-N')Pt(Me)(MeCN)⁺ (C). (c) Time scale: 7 min. Experimental conditions: [Pt^{II}] = 0.125 mM, [MeCN] = 5.74 M (30%), and [HBF₄·Et₂O] = 1 mM.

The kinetics of the methane-releasing reaction step, $k_{\text{obs}}(\text{elim})$, were studied as a function of the acid and MeCN concentrations within the temperature range of -40 to +10 °C. The time-resolved spectra were fitted to a single-exponential function that resulted in $k_{\text{obs}}(\text{elim})$ values. The rate of this methane release shows no acid concentration

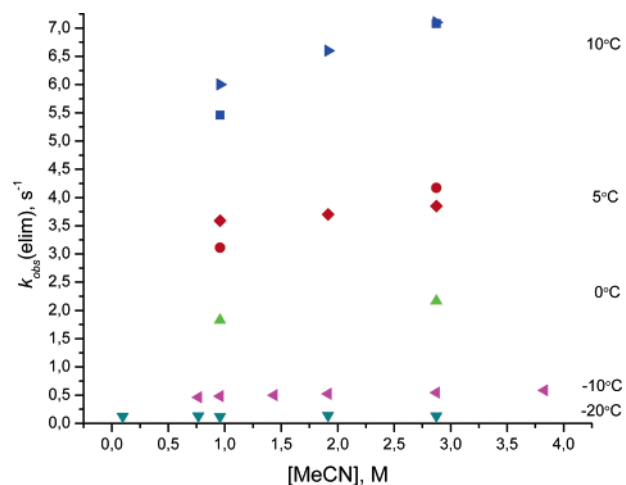


Figure 6. $k_{\text{obs}}(\text{elim})$ for the methane elimination vs [MeCN] for the reaction in CH₂Cl₂. Experimental conditions: [Pt^{II}] = 0.125 mM, [HBF₄·Et₂O] = 1 mM, and $T = -40$ to +10 °C.

Table 1. Kinetic Data for the Second Step of the Reaction between (N'-N')PtMe₂ and HBF₄·Et₂O in CH₂Cl₂ as a Function of Pressure^a

P (MPa)	$k_{\text{obs}}(\text{elim})$ (s ⁻¹)
8	3.7 ± 0.2
50	2.7 ± 0.1
90	2.0 ± 0.1
130	1.43 ± 0.04
$\Delta V^\ddagger = +18 \pm 1 \text{ cm}^3 \text{ mol}^{-1}$	

^a Experimental conditions: [Pt^{II}] = 0.125 mM, [MeCN] = 5.74 M, [HBF₄·Et₂O] = 1 mM, and $T = 5$ °C.

dependence, as might be anticipated. However, somewhat surprisingly, the MeCN concentration also does not significantly affect the reaction rate. The dependence of $k_{\text{obs}}(\text{elim})$ on [MeCN] as a function of temperature is shown in Figure 6. Only a slight MeCN dependence was observed at the highest applied temperature (+10 °C), which probably results from a medium effect. From the average values of measured $k_{\text{obs}}(\text{elim})$ at each temperature (Table S2 in the Supporting Information), the activation parameters for the second reaction step were found to be $\Delta H^\ddagger = 75 \pm 1 \text{ kJ mol}^{-1}$ and $\Delta S^\ddagger = +38 \pm 5 \text{ J mol}^{-1} \text{ K}^{-1}$. The kinetics of this step were furthermore monitored at elevated pressures at 5 °C for a solution containing 30% MeCN by volume. From the good linear correlation between $\ln[k_{\text{obs}}(\text{elim})]$ and the pressure data summarized in Table 1, the activation volume was found to be $\Delta V^\ddagger = +18 \pm 1 \text{ cm}^3 \text{ mol}^{-1}$. The high activation enthalpy, large positive value of the activation entropy, and large positive volume of activation strongly suggest a dissociative character of the rate-limiting step for the methane-releasing reaction.

The reaction between (N'-N')PtMe₂ and HBF₄·Et₂O was investigated at room temperature in a tandem cuvette. The Pt complex was dissolved in neat CH₂Cl₂ and mixed with the acid at a constant concentration in MeCN/CH₂Cl₂ solvent mixtures of different [MeCN]. No observable changes were seen in the spectra after mixing of the reactants when [MeCN] was varied. At the same time, although the spectrum of the product and the rate constants for the product formation at different temperatures were not affected by varying the MeCN concentration, significant differences were

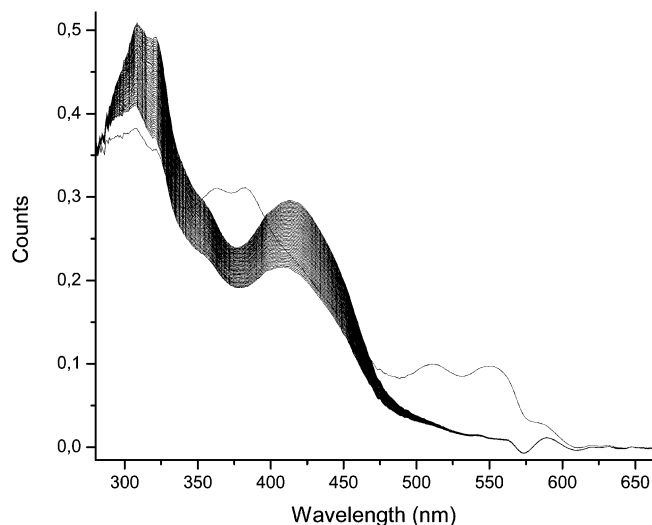
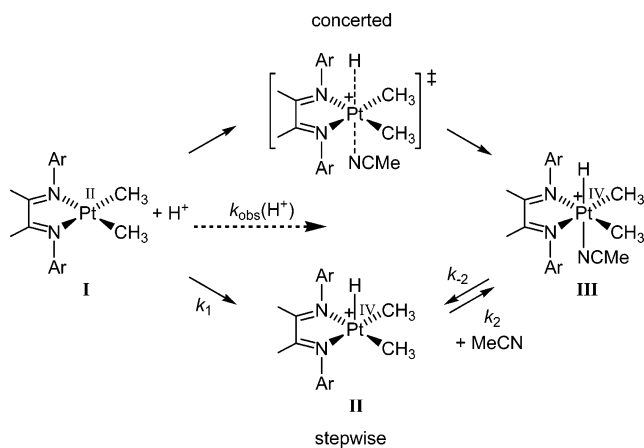


Figure 7. Time-resolved spectra for the reaction of $(N'-N')PtMe_2$ with $HBF_4 \cdot Et_2O$ in CH_2Cl_2 at $-40^\circ C$. Experimental conditions: $[Pt^{II}] = 0.125$ mM, $[MeCN] = 0.96$ M (5%), and $[HBF_4 \cdot Et_2O] = 1$ mM. Time scale: 1 min.

seen in an intermediate spectrum, which is characteristic for the Pt^{IV} species that is formed between the protonation step and the subsequent reductive elimination. In the presence of higher $[MeCN]$ at $-40^\circ C$ (Figure 5), the spectroscopic signature of the intermediate, identical with that of the platinum(IV) hydrido product of the protonation step at lower temperatures (Figure 1), is detected. At the same temperature and $[HBF_4 \cdot Et_2O]$ but at low $[MeCN]$, the intermediate Pt^{IV} species can no longer be clearly observed (Figure 7). The calculated spectra of the species involved in the overall reaction under these conditions and the time-resolved spectra on the longer time scale are shown in Figure S1 in the Supporting Information. After the initial rapid protonation, the starting spectrum for the following step immediately assumes the characteristics of the product $(N'-N')Pt(Me)(NCMe)^+$, and the overall reaction appears to proceed without passing through an observable intermediate. This effect is more prominent at higher temperatures (Figure S2 in the Supporting Information). There may be two important reasons for this behavior. The first is the fact that the protonation step has a very low activation enthalpy compared to the reductive elimination. This results in a dramatic acceleration of the methane elimination relative to the initial protonation when the temperature is raised and, eventually, the elimination starts to interfere with the protonation kinetics. This occurs most notably at low $[MeCN]$, where the first step is slowed at lower $[MeCN]$, as was discussed above (see the discussion of Figure 4). The second reason is that at lower $[MeCN]$ the formation of the hexacoordinate Pt^{IV} intermediate is less efficient because of competing reductive $H-CH_3$ coupling and methane loss, which is consistent with the previously reported NMR studies.

Suggested Mechanism. The results of the present kinetic investigation are fully consistent with the previously proposed mechanism¹⁵ (Scheme 3) in which the putative (unobserved) pentacoordinate platinum(IV) hydrido complex is trapped by a solvent molecule and/or undergoes reductive C–H cou-

Scheme 4



pling. In principle, each of the reactions for which kinetics are reported here may or may not proceed via the hexacoordinate intermediate. This will be taken into account, and for clarity the two reactions—the protonation of **I** to produce **III** and the methane elimination from **III** to produce **V**—will be discussed separately.

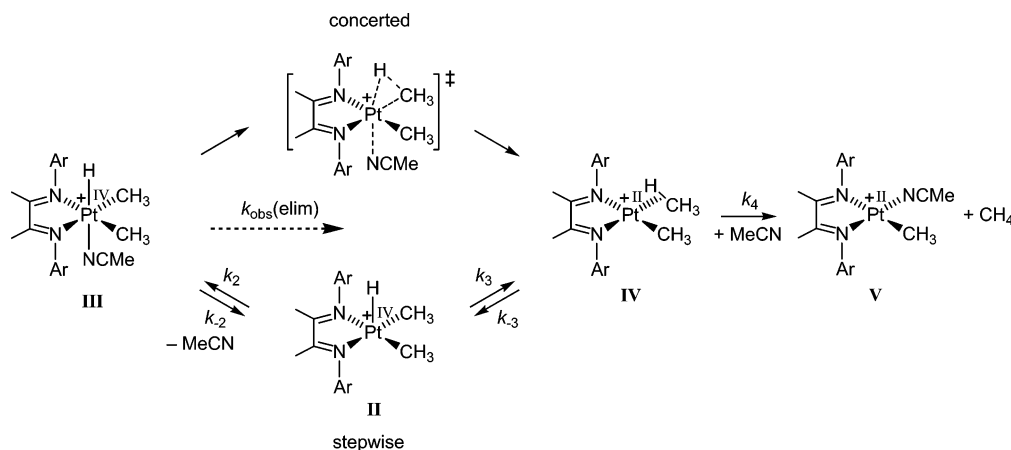
The protonation reaction, which proceeds with an experimentally determined rate $k_{obs}(H^+)$, can be presented by Scheme 4. The top pathway represents a concerted protonation/MeCN coordination that does not involve the pentacoordinate intermediate. The transition state comprises the starting Pt^{II} complex, a proton, and a MeCN molecule and should ideally be first-order with respect to each component. The protonation kinetics at $-78^\circ C$ are zero-order in $[MeCN]$ over a wide concentration range, and this strongly argues against the concerted pathway. The stepwise path is consistent with the low-temperature kinetics, provided that the addition of the proton, i.e., k_1 , is rate-limiting and the MeCN addition k_2 is fast. At $-78^\circ C$, the platinum(IV) hydride is stable and k_{-2} (which produces **II**, the putative intermediate also for the elimination of methane) is slow.⁴²

Two alternative pathways for the methane elimination reaction, which proceeds with the experimentally measured rate $k_{obs}(elim)$, are depicted in Scheme 5. The bottom path involves initial MeCN dissociation (k_{-2}) to form the pentacoordinated intermediate **II**, which yields the σ complex **IV** after C–H reductive coupling. The top path is a concerted process that furnishes the same σ -complex intermediate. Both alternatives are dissociative with respect to MeCN; they only differ in the timing of the MeCN release relative to C–H coupling.⁴³ Reductive X–Y eliminations from octahedral $L_2-Pt^{IV}(X)(Y)$ compounds are usually considered to be dissociative if a readily dissociable ligand is present; whether the overall process occurs in a concerted or stepwise fashion is

(42) A third alternative in which MeCN addition precedes protonation may also be discounted on the basis of zero-order MeCN dependence: First-order kinetics with respect to $[MeCN]$ should arise whether MeCN addition is rate-limiting or in preequilibrium with rate-limiting protonation.

(43) A third alternative that produces **V** directly from **III** in a concerted reductive elimination/MeCN dissociation bypasses both intermediates **II** and **IV**. This alternative is discounted on the basis of the substantial body of experimental evidence that implies complexes akin to **IV** in C–H activation and reductive elimination chemistry at Pt.^{8,9}

Scheme 5



strongly dependent on the nature of X, Y, and the supporting ligands L.^{8,9,44,45} (An interesting consequence, imposed by the principle of microscopic reversibility, of a concerted process would be that isotopic exchange between hydrido and methyl sites at Pt, which proceeds by methane “rotation” at **II**, would require transition-state stabilization by a donor ligand, in this case MeCN.)

The putative pentacoordinate species **II** is a common intermediate for the protonation (Scheme 4) and elimination (Scheme 5) reactions. There have been no direct observations of **II** in any previous experiments. There is also no direct evidence for the discrete pentacoordinate hydrido species **II** in the rapid-scan experiments reported here, but we note that a few relatively stable, neutral pentacoordinate platinum-(IV) alkyl complexes have been recently reported.^{46–49} The hexacoordinate species **III** is stable at $-78\text{ }^{\circ}\text{C}$ under the rapid-scan conditions and does not convert to **V** on the time scale of the experiment (30 min). Under the NMR conditions at this temperature, **V** is formed, in part, during the protonation, most notably at low [MeCN].¹⁵ At higher [MeCN], the formation of **III** predominates. Protonation at low [MeCN] will favor k_3 over $k_2[\text{MeCN}]$ (see Scheme 3) to produce a mixture of **III** and **V**. There is a possibility that step 3, reductive coupling/oxidative cleavage, might be reversible; i.e., k_3 and k_{-3} are both kinetically significant. This scenario should give rise to H/D scrambling between hydrido and methyl sites in a reaction between $(N'-N')\text{Pt}(\text{CH}_3)_2$ and deuterated acid and would be detected by the generation of the ^1H NMR-observable scrambling product $(N'-N')\text{Pt}(\text{CH}_2\text{D})(\text{NCMe})^+$ after the associative methane displacement¹³ from **IV** by MeCN. This possibility was investigated under relevant reaction conditions (see the Experimental Section). The absence of the Pt- CH_2D NMR

resonance that would signal the scrambling product suggests that the reductive coupling k_3 is essentially irreversible under the actual reaction conditions of this study (unless coupling exhibits a substantial isotope effect that would serve to attenuate the extent of scrambling). The ^1H NMR spectrum showed that CH_4 as well as CH_3D were formed in this experiment. The presence of CH_4 is not at odds with the lack of Pt- CH_2D because CH_4 would always arise from unavoidable traces of protic contaminants (see the Experimental Section). It should be pointed out that under quite different reaction conditions (trifluoroethanol- d_3 solvent, ambient temperature) extensive H/D scrambling between hydrido and methyl sites was seen when $(N'-N')\text{Pt}(\text{CH}_3)_2$ was treated with DOTf.¹³ This suggests that a more polar solvent could promote scrambling by assisting proton transfer or by stabilizing the pentacoordinate Pt^{IV} intermediate and making the reaction step **II** \rightarrow **IV** reversible.

At higher temperatures, the subsequent reductive elimination of methane is observed in the stopped-flow experiments. The measured rate constant $k_{\text{obs}}(\text{elim})$ of this reaction is independent of [MeCN], suggesting that k_{-2} must be the rate-determining step, followed by the rapid reaction sequence **II** \rightarrow **IV** \rightarrow **V**. The combined kinetic experiments have established that the protonation, $k_{\text{obs}}(\text{H}^+)$, proceeds with a relatively low ΔH^\ddagger of ca. 15 kJ mol^{-1} , whereas the reductive elimination, $k_{\text{obs}}(\text{elim})$, has a ΔH^\ddagger value of ca. 75 kJ mol^{-1} . When the temperature is raised, $k_{\text{obs}}(\text{elim})$ will therefore be accelerated to a much greater extent than $k_{\text{obs}}(\text{H}^+)$. Thus, whereas $k_{\text{obs}}(\text{H}^+) \gg k_{\text{obs}}(\text{elim})$ at $-78\text{ }^{\circ}\text{C}$, i.e., the platinum-(IV) hydrido complex is relatively stable because of slow $k_{\text{obs}}(\text{elim})$, the converse is true at elevated temperatures and therefore the platinum(IV) hydrido complex cannot be observed at the higher temperatures. Under such conditions, k_3 must be $\gg k_2[\text{MeCN}]$; if this is not the case, the observed rate constant should show a significant [MeCN] dependence. Figure 6 illustrates how $k_{\text{obs}}(\text{elim})$ slightly increases with increasing [MeCN], whereas, in fact, an increase in [MeCN] should cause a decrease in $k_{\text{obs}}(\text{elim})$ according to the rate law presented in eq 1. Such behavior was recently observed in related work on a pyridine-coordinated complex.⁵⁰ If the

(44) Arthur, K. L.; Wang, Q. L.; Bregel, D. M.; Smythe, N. A.; O'Neill, B. A.; Goldberg, K. I.; Moloy, K. G. *Organometallics* **2005**, *24*, 4624–4628.

(45) Crumpton-Bregel, D. M.; Goldberg, K. I. *J. Am. Chem. Soc.* **2003**, *125*, 9442–9456.

(46) Reinartz, S.; White, P. S.; Brookhart, M.; Templeton, J. L. *J. Am. Chem. Soc.* **2001**, *123*, 6425–6426.

(47) Fekl, U.; Kaminsky, W.; Goldberg, K. I. *J. Am. Chem. Soc.* **2001**, *123*, 6423–6424.

(48) Fekl, U.; Goldberg, K. I. *J. Am. Chem. Soc.* **2002**, *124*, 6804–6805.

(49) Fekl, U.; Kaminsky, W.; Goldberg, K. I. *J. Am. Chem. Soc.* **2003**, *125*, 15286–15287.

(50) Procelewska, J.; Zahl, A.; Liehr, G.; van Eldik, R.; Smythe, N. A.; Williams, B. S.; Goldberg, K. I. *Inorg. Chem.* **2005**, *44*, 7732–7742.

$$k_{\text{obs}}(\text{elim}) = \frac{k_{-2}k_3 + k_{-3}k_2[\text{MeCN}]}{k_3 + k_2[\text{MeCN}]} \quad (1)$$

reaction from **II** to **IV** is irreversible as supported by the NMR experiment described above, this rate expression simplifies to eq 2; furthermore, if $k_3 \gg k_2[\text{MeCN}]$, it reduces to $k_{\text{obs}}(\text{elim}) = k_{-2}$. This is entirely consistent with the positive activation entropy and activation volume values found for $k_{\text{obs}}(\text{elim}) (=k_{-2})$ under these conditions.

$$k_{\text{obs}}(\text{elim}) = \frac{k_{-2}k_3}{k_3 + k_2[\text{MeCN}]} = k_{-2} \quad (2)$$

The rapid-scan experiments at $-40\text{ }^\circ\text{C}$ also show the formation of **III** and **V** in the same time interval, in good agreement with NMR observations. At higher $[\text{MeCN}]$, the rapid-scan experiments at $-40\text{ }^\circ\text{C}$ and higher temperatures clearly show the formation of **III** (Figure 5) as observed at $-78\text{ }^\circ\text{C}$, whereas at lower $[\text{MeCN}]$, the overall reaction proceeds more through the direct **I** \rightarrow **II** \rightarrow **IV** reaction sequence (Figure 7) than through the **I** \rightarrow **III** \rightarrow **II** \rightarrow **IV** sequence.

Conclusions

In this paper, the results from rapid-scan UV–vis spectroscopic measurements on the protonation and subsequent methane-release reaction of a (diimine)platinum(II) dimethyl complex within the temperature range of -90 to $+10\text{ }^\circ\text{C}$ were reported. In combination with the results of previously reported NMR studies, this study provides a more complete

and quantitative picture of two important reactions, protonation/deprotonation at the metal center and C–H bond formation, which are relevant to C–H activation at Pt. Kinetic and activation parameters obtained for the two well-separated reaction steps clearly suggest the oxidative addition and reductive elimination character of the two studied processes. These results are quite unique because kinetic studies on protonation reactions at metals are rather rare, and its spectral visualization is difficult because of their rapid nature. Although in the time-resolved UV–vis spectra there is no direct evidence for the existence of the pentacoordinate platinum(IV) hydrido complex, the agreement between stopped-flow and NMR results supports the mechanism in which it is the pentacoordinate intermediate that undergoes reductive elimination. The formation of the crucial pentacoordinate species proceeds by rate-limiting dissociation of the apical ligand MeCN from the hexacoordinate Pt^{IV} complex. In a recent report on a closely related system, it was clearly shown that ligand dissociation induces reductive C–C coupling,⁵⁰ which is in full agreement with the findings of this study.

Acknowledgment. We gratefully acknowledge generous financial support from the Norwegian Research Council and the Deutsche Forschungsgemeinschaft and also DAAD for providing travel support.

Supporting Information Available: Three figures presenting rapid-scan spectroscopic data and two tables with kinetic data as a function of temperature. This material is available free of charge via the Internet at <http://pubs.acs.org>.

IC0519537